IOPscience iopscience.iop.org

Home Search Collections Journals About Contact us My IOPscience

(100) GaP surface charges, potentials, and stoichiometry; a quantum-chemical study

This article has been downloaded from IOPscience. Please scroll down to see the full text article.

1994 J. Phys.: Condens. Matter 6 4255

(http://iopscience.iop.org/0953-8984/6/23/005)

View the table of contents for this issue, or go to the journal homepage for more

Download details:
IP Address: 171.66.16.147
The article was downloaded on 12/05/2010 at 18:33

Please note that terms and conditions apply.

J. Phys.: Condens. Matter 6 (1994) 4255–4268. Printed in the UK

(100) GaP surface charges, potentials, and stoichiometry; a quantum-chemical study

E V Stefanovich†‡ and A L Shluger†‡

† The Royal Institution of Great Britain, 21 Albemarle Street, London W1X 4BS, UK
‡ Department of Chemical Physics of Condensed Matter, University of Latvia, 19 Rainis Boulevard, Riga LV-1098, Latvia

Received 9 December 1993, in final form 28 February 1994

Abstract. We studied the charge and potential distribution near the (100) GaP surfaces which bear the characteristic features common to polar surfaces of semiconductors. A self-consistent periodic quantum-chemical technique and a slab model are employed and the atomic and electronic structures for several surface stoichiometries are calculated. We compare these results with the predictions of the model approaches in order to check the limits of applicability of simplified models such as the electron–hole counting model or the model suggested by Nosker, Mark and Levine. We have found that zero dipole moment of the slab is an important criterion of the surface stability. The charges of the surface ions are flexible in our model and decrease strongly at the surface with respect to the bulk values. Therefore this criterion does not impose such severe restrictions on the surface stoichiometry, composition, and structure as are suggested in other models. We conclude that structure and stability of polar surfaces are determined by a balance of stoichiometric factors and electron density redistribution which should both be taken into account in a self-consistent manner.

1. Introduction

The surfaces of III–V semiconductors crystallizing with the zincblende structure have been the topic of extensive experimental studies. These compounds belong to a wide class of heteropolar semiconductors. An important feature of these compounds is that their electronic stucture may be characterized by a certain degree of ionicity. The (100) surfaces are usually grown using molecular–beam epitaxy (MBE) or similar techniques and may be thought of as a termination of a sequence of alternating charged layers of anions and cations. Therefore these crystal faces are polar and have properties different from those characteristic to neutral (110) surfaces of the same compounds. The structure of the upper layers forming the surface differs considerably from an ideal (100) cut of the bulk material. A wide variety of different reconstructions and surface compositions has been observed experimentally at different temperatures [1]. However, the details of atomic and electronic structures for the majority of the surface reconstructions are still unclear.

Model approaches proved to be very useful for qualitative analysis and prediction of stable surface structures. We will mention two of them that use different models for charge distribution within the crystalline lattice, both in the bulk and near the surface. In particular, most of the recent results have been obtained within a covalent model which allows dangling bonds at the surfaces. On the other hand, as was emphasized by Nosker, Mark and Levine [2] (NML model) even small electron transfer between atoms in zincblende lattices is important in

0953-8984/94/234255+14$19.50 © 1994 IOP Publishing Ltd

interpreting surface effects because of electrostatic (Madelung) contribution to the surface energy. Both of these arguments, if taken separately, impose severe restrictions on the surface stoichiometry, structure and potential distribution [2–6], and the predictions of the two models with regard to these surface properties differ markedly.

Contradictions between different models can be resolved with an aid of fully self-consistent model-independent quantum-mechanical calculations of the electronic and atomic structures of the polar surfaces [7]. Polar surfaces of III–V semiconductors have already been the topic of extensive quantum-mechanical studies. In particular, tight-binding [8–12] and pseudopotential LDF calculations [13–18] have been performed for (100) and (111) surfaces of GaAs using a slab model. However, in most of these calculations an artificial change of the valence charge of the surface (interface) atoms or symmetry restrictions were imposed in order to prevent a 'charge transfer' between opposite faces of the calculated slabs. Also, the tight-binding method does not allow for self-consistency between the surface charges and potentials (some attempts to overcome this difficulty were made in [19]). Thus global optimization of electronic and atomic structures of the polar surfaces of semiconductors remains a complicated problem.

In this paper we employed an MO LCAO Hartree–Fock–Roothaan technique within a large-unit-cell (LUC) model of a periodic slab with a particular aim to take into account the electron density and potential distribution inside the slab in a self-consistent way. This method also allows us to calculate the surface atomic and electronic structures. To study the dependence of these characteristics on the slab thickness one should use periodic cells of more than 70 atoms. Therefore the approximation of intermediate neglect of differential overlap (INDO) was imposed on the elements of the Fock matrix. Because of the approximate nature of this study we focus mainly on a qualitative features of charge and potential distribution near polar surfaces of GaP. The latter bear features common to polar surfaces of III–V semiconductors. We compare our results with the predictions of the model approaches in order to check the limits of applicability of the simplified models. Particular properties of the GaP surfaces are interesting from a general point of view and because of photo-induced processes found experimentally in recent studies [20]. Investigation of the micro-mechanisms of these processes determines further goals of our studies.

The paper is organized as follows. In section 2 several models of polar surfaces widely used in the literature are reviewed. We pay particular attention to the values of the surface charge and dipole moment predicted by these models. In section 3 the computational method is described. In section 4 the surface charge and potential distributions are analysed for P-terminated surfaces with 2:4, 3:4, and 4:4 stoichiometries. These properties were calculated taking into account the relaxation and reconstruction of the surface layer. The results regarding surface geometry and desorption energy of the P and Ga dimers are also presented. The results of calculations are discussed and compared with the existing models in section 5.

2. Models of polar surfaces

The choice of the surface model is particularly important for the study of polar surfaces. Polar surfaces usually have large formation energies and cannot be obtained as a cleavage planes of massive crystals. In particular, the (100) surfaces of III–V semiconductors, which are usually grown by means of the MBE technique, form thin films on the substrate. The model of the slab finite in the z direction and having 2D periodicity in the x and y directions seems to be most appropriate to describe these surface structures. We should note that a model of a slab periodically repeated in the z direction, which is often used in surface

studies [14, 16, 17], is generally not appropriate for polar surfaces. The reason is that the charge distribution in the polar slab may create a spurious dipole moment in the z direction [2, 3], and as a consequence the potential distribution may not be z periodic. To avoid charge-transfer problems between surfaces Qian *et al* [15] in their recent calculations of stoichiometry and surface reconstruction of the (001) GaAs surfaces imposed an artificial fractional charge on one end of the slab. A layer of fictitious H atoms terminating one side of the slab was used by Ohno [17].

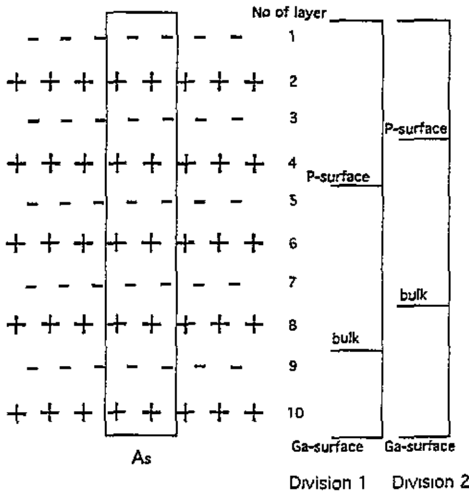

Figure 1. Schematic diagram of the slab representing the polar GaP(100) surface. The surface unit cell is denoted by lines; A_s is the area of the unit cell. Division 1 of the slab into the 'P surface', 'bulk', and 'Ga surface' regions was employed in the present study to define the surface charges (see table 1). Division 2 is equivalent to division 1 but leads to different values of the surface charges (see section 5).

It is convenient to employ the same surface model for discussion of the model approaches and further comparison with the results of the present calculations. For this purpose we will use a slab consisting of 10 GaP(100) layers, which is schematically presented in figure 1. The top layer of the slab consists of anions (in our case the P atoms), whereas the bottom layer consists of cations (the Ga atoms). Generally, the slab can be divided into three regions: P surface, bulk, and Ga surface. This division is conditional and is discussed in more detail in sections 4 and 5. Let us suppose for the present discussion that the P surface consists of surface layers 1–4, the bulk of 5–8, and the Ga surface of surface layers 9 and 10 (see division 1 in figure 1). We will refer to the *sum* of the charges of ions in the P surface and in the Ga surface regions calculated per 2×1 surface unit cell as the *surface charges* Q_P and Q_{Ga} respectively. For the thick enough slabs the bulk region may be constructed of an integer number of bulk unit cells and the total charge of the bulk region is equal to zero. In this case $Q_P = -Q_{Ga}$. The moduli of the charges on the bulk ions are denoted as q_b, and the total dipole moment of the (slab) unit cell as D. Note that the definition of the *total* dipole moment is unambiguous, since the total charge of the unit cell is zero. The dipole moment of the slab is related to the difference in the electrostatic potentials on the two sides of the slab by

$$4\pi D/A_s = \phi \,|_{z=-\infty} - \phi \,|_{z=\infty} \tag{1}$$

where A_s is the area of the surface unit cell (see figure 1).

In some approaches, such as those used in atomistic simulation of surfaces, it is often assumed that charges on the surface ions are equal to those in the bulk [21] which is a reasonable approximation for ionic crystals (see, for example, [22]). Another common assumption (see, for example, [10, 13, 16]) is that an unrelaxed surface can be treated as an

ideal termination of the bulk structure. (In further discussion we will refer to this model as a 'bulk cut' model.) For the above described division of the slab into the bulk and surface regions this immediately leads to zero surface charges and a dipole moment of the slab which increases proportionally to the slab thickness d. The average potential distribution inside the slab in this model will depend linearly on the z coordinate and an unphysical situation may occur in which the potential is positive (negative) on cations (anions).

Intuitively, this situation is highly unstable. As was suggested by Nosker, Mark and Levine [2] (NML model), the two faces of the surface slab must bear opposite charges in order to restore a more realistic potential distribution. In the case of the (100) surface of the zincblende crystal the surface charges should be $Q_{Ga} = -q_b$, $Q_P = q_b$. Since the ionic charges are assumed to be fixed in this model, changes in the surface stoichiometry (and structure) are proposed to be responsible for the creation of the surface charge. The simplest surface structure predicted by this model corresponds to the 1:2 stoichiometry for both Ga- and P terminated (100) GaP surfaces.

Another model, the so-called electron–hole counting (EHC) model [4, 5] is based on the three following assumptions: (i) a completely covalent model of chemical bonding in the bulk of the crystal (zero ionic charges); (ii) non-conducting character of the stable surfaces; (iii) pure anionic (cationic) character of the filled (empty) dangling bond surface bands. To fulfil all these conditions it is proposed that electron transfer should occur between the surface Ga and As atoms to fill the dangling bonds on the surface anions while leaving the dangling bonds on the surface cations empty. The surface structures failing to satisfy this electron counting rule are predicted to be unstable. The restrictions on the surface stoichiometry and structure imposed by this model are generally different from those arising from the NML model. In particular, the 3:4 'missing-dimer' geometry of the P-terminated (100) surface was predicted to be stable on its basis [4]. Although the bulk dipole moment and the surface charges are zero in this model, due to charge transfer on the surface the surface atoms bear non-zero charges. For instance, P atoms on the (100) surface have 5.75 valence electrons ($\frac{5}{4}$ electrons on each of the three P–Ga bonds and two electrons on the filled dangling bond) and an ionic charge of -0.75. Ga atoms on the surface bear the ionic charge 0.75. Therefore the whole slab has a non-zero dipole moment and hence the electrostatic potentials on the two sides of the slab are different.

The bulk ionicity was taken into account in the generalization of the EHC model proposed by Harrison [3]. In this model the surfaces bear a non-zero charge in order to have zero dipole moment of the slab as in the NML model. In both the EHC and Harrison's models, the charges of surface ions are greater than those in the bulk. They depend only on the number of dangling bonds (i.e. coordination number) of the surface ions. Due to the restrictions imposed on the surface ionic charges, Harrison's model also leads to severe constraints on surface composition and structure.

The basic features of the models discussed above are summarized in table 1. In all model approaches only a limited number of surface structures and stoichiometries satisfies the imposed constraints. Therefore it seems difficult to explain gradual growth of the (100) GaAs or GaP surfaces by the modern layer-by-layer MBE technique [23, 24] (see, however, discussion on the EHC model in [4]). As has been pointed out in [23], although the basic structure predicted by the EHC model for the (100) GaAs surfaces, the 'missing-dimer' model, has been confirmed by scanning-tunnelling-microscope observation [31], it has not yet proved possible to image filled As-related and empty Ga-related states. Therefore there is no confirmation of the basis of the EHC model, even under static conditions. The present state of affairs can be characterized therefore from two points of view: (i) experimentally, there is a problem in the understanding of both static and dynamic conditions of MBE

Table 1. Comparison of different models for the GaP(100) surface. DB stands for dangling bonds. The surface charge is calculated for the 2×1 unit cell. For the definition of the surface regions see the text and figure 1. The entries which are the basic statements of the models are emphasised in bold.

	Model of the surface				
Surface property	'Bulk cut'	NML	EHC	Harrison's	This work
Ionicity	**constant**	**constant**	increase	increase	decrease
Occupancy of DB (P)	partial[a]	partial[a]	**filled**	**filled**	partial
Occupancy of DB (Ga)	partial[a]	partial[a]	**empty**	**empty**	partial
Surface charge	**0**	$\pm q_b$	**0**	$\pm q_b$	$\pm q_b$
Slab dipole moment	$q_b d$	**0**	non-zero	**0**	**0**

[a] In both 'bulk cut' and NML models the electron occupancy of the dangling bonds is not explicitly specified; however conservation of the bulk ionicity implies that both Ga and P dangling bonds on the surface should be partly occupied by electrons.

growth of polar surfaces [23, 24]; (ii) theoretically, there are difficulties in treating polar surfaces using atomistic simulation, tight-binding and some of the band-structure calculation techniques due to the very large dipole moment of the slab. The results of calculations presented in the next sections support some of the predictions of the EHC model. They demonstrate, however, that a realistic model approach to the understanding of the properties of polar surfaces of semiconductors should accurately take into account the charge and potential distribution in these systems.

3. Computational technique

We use the LUC model and the self-consistent semi-empirical INDO method [25] which were modified in previous works [26, 27] to provide a better description of the structural and electronic properties of ionic and semi-covalent crystals and their surfaces. The basic idea of the LUC model consists in computing the electronic structure of the unit cell extended in a special manner (large unit cell) at $k = 0$ in the narrowed Brillouin zone (NBZ). This is equivalent to a band calculation at those BZ k points which transform to the NBZ centre on extending the unit cell. In particular, 2×4 extension of the (100) GaP surface unit cell used in the present work is equivalent to the band structure calculation at eight k points in the BZ. This technique was extensively used for defect studies in ionic crystals (see, for example, [28]); defects in silicon [29] were also successfuly studied by this method. This method is realized in the CLUSTER computer code. In the INDO method some of the elements of the Fock matrix are calculated using numerical parameters [26, 27]. The INDO parameters for the H atom (used in the calculations for the PH_3 and GaH_3 molecules) were taken from [27]. The INDO parameters for the Ga and P atoms were fitted for the present study. We sought a compromise set of Ga and P parameters which would represent the most important characteristics of the electronic and geometrical structures of atoms, Ga- and P-containing molecules, the GaP crystal, and the GaP(110) surface. The method of optimization of the parameters was essentially the same as described in [27]. The electronic configurations of P and Ga atoms on the (110) surface of the GaP crystal are believed to be very similar to those in the PH_3 and GaH_3 molecules [30]. By analogy with the well studied dimerization of the GaAs(100) surface [11, 17, 31, 32], we can assume that the chemical bonding on the GaP(100) surface resembles that in the P_2 and Ga_2 molecules. Therefore, the parameters were fitted to describe also the properties of these molecules [33, 34]. The final set of

parameters is given in tables 2 and 3.

Table 2. One-centre INDO parameters. Conventional definition of the parameters is used [27, 25].

	Ga	P	H
ζ_s (a.u.)	1.59	1.78	1.2
ζ_p (a.u.)	1.24	1.78	—
E_s (eV)	9.85	15.0	4.0
E_p (eV)	0.6	4.2	—
$-\beta_s$ (eV)	1.0	9.0	2.0
$-\beta_p$ (eV)	4.5	15.0	—
P_{0s}	2.0	2.0	0.8
P_{0p}	0.333	1.0	—

Table 3. Two-centre INDO parameters of the electron–core interaction (a.u.). See [26] for more details.

	B		
A	Ga	P	H
Ga	0.0	0.0	0.23
P	0.15	0.0	0.1
H	0.23	0.1	0.4

As a test of the ability of the derived set of parameters to reproduce the relative balance between the Ga–Ga, Ga–P, and P–P interactions, we performed extensive calculations for the Ga_2P_2 molecule in different conformations. These results can be compared with the results of *ab initio* calculations of the similar Ga_2As_2 molecule [35] (see table 4). Although direct comparison is impossible, one can see that general trends in energetics and geometrical structure are very similar in the two molecules.

Table 4. Ga_2P_2 molecular properties. *Ab initio* results [35] refer to the Ga_2As_2 molecule. Abbreviations for the molecular structures are taken from [35]. Numbers in parentheses correspond to incompletely optimized geometries.

		Distances						Relative energies (eV)	
		CLUSTER (INDO)			*Ab initio* [35]				
Structure	State	P–P	Ga–P	Ga–Ga	As–As	Ga–As	Ga–Ga	INDO	[35]
rhombic	^1A_g	3.94	5.01	—	4.50	5.18	—	0	0
	^3A_u	3.98	5.10	—	5.13	4.84	—	0.27	0.91
$T_{Ga-P(As)_2}$	$^1A_1$	3.70	5.04	5.44	4.49	4.72	5.30	1.85	0.95
cis-form	$^3B_1$	3.90	5.06	5.98	4.73	4.73	5.69	1.41	1.14
	$^1A_1$	3.86	4.85	6.14	4.52	4.98	6.46	2.69	1.19
linear c;ac	$^3\Sigma_g^-$	3.98	4.78	—	4.43	4.78	—	3.24	1.87
$T_{P(As)-Ga_2}$	$^1A_1$	3.84	4.69	6.90	(4.2)	(5.4)	(5.8)	3.30	unstable

[a] Ga–P–P–Ga (Ga–As–As–Ga) geometry.

Table 5. Comparison of GaP bulk crystal properties calculated in this work with the 48-atom LUC and obtained in other studies. a_0 is the lattice constant in Å, BE is the binding energy per atom couple, E_g is the band gap; E_v is the total valence band width (the energy difference between Γ_{15} and Γ_1 symmetry points (zincblende notation see [41])); E_{vs} is the width of the valence 's sub-band' ($\varepsilon_{X_1} - \varepsilon_{\Gamma_1}$); E_{vp} is the width of the valence 'p sub-band' ($\varepsilon_{\Gamma_{15}} - \varepsilon_{X_3}$); all energetic parameters in eV.

Property	CLUSTER	Other data
a_0	2.70	2.72 [39]
BE	9.8	7.3 [39]
E_g	4.46	2.39 [40]
E_v	14.7	13.1 [41]; 12.5 [40]
E_{vs}	3.3	3.8 [41]; 2.93 [40]
E_{vp}	8.7	7.1 [41]; 6.4 [40]
q_b	1.07	0.75 [40]

In all cases the calculated P–P distances are on average 15% shorter than the corresponding As–As distances computed in [35]. This is easy to understand because the P–P equilibrium distance in the P_2 molecule is approximately 10% shorter than that in the As_2 molecule (2.11 Å [35]). The calculated Ga–P and Ga–Ga distances agree with the results for Ga–As and Ga–Ga [35] with an accuracy of better than 7%. The relative energies of different Ga_2P_2 structures are reproduced correctly except for inversion of the order of the T $GaAs_2$ structure and the *cis*-form in the triplet state. The calculated energy separations between different geometries are larger than those for the Ga_2As_2 molecule. The latter can be easily understood since the P–P and Ga–P bonds are known to be stronger than As–As and Ga–As bonds [33, 35, 36].

The atomic and electronic structures of perfect crystals and crystal surfaces were studied using a large-unit-cell (LUC) model described in [37]. The surface properties were calculated with a single-slab model. We assume that the surface is non-magnetic, i.e. corresponds to the perfect pairing of electrons with opposite projections of spin. Therefore the restricted Hartree–Fock method was used in all further calculations. The existence of magnetic surfaces cannot be, however, ruled out completely (see, for example, [7, 38]). The unrestricted Hartree-Fock method should be used to study a spin density distribution in this case.

For the (110)GaP surface the calculated slab consisted of six atomic layers. The surface LUC (translation vectors $a_1 = a_0(0, 2\sqrt{2}, 0)$ and $a_2 = a_0(4, 0, 0)$, where a_0 is the bulk lattice constant) is obtained as the 2×2 extension of the minimal surface UC and consists of 48 atoms. The positions of the atoms in the top and bottom surfaces were optimized independently. The lattice constant, a_0, in the surface calculations was taken to be the same as that optimized for the bulk (see table 5). In the bulk calculations the same 48-atom LUC was used but with 3D translations a_1, a_2, and $a_3 = a_0(0, 0, -3\sqrt{2})$.

The calculated properties of the GaP bulk crystal are presented in table 5 and compared with the results of other calculations. The one-electron energy gap E_g presented in the table is larger than the experimental value. The value of E_g calculated using a configuration interaction technique and taking into account only the one-electron excitations is 2.9 eV. It must be reduced even more strongly if electron correlation is included in the consideration. For the moment this has been done only for the ground state properties of GaP [39]. The value of the correlation correction is not yet established for the GaP crystal. Ionic charges were calculated using Lowdin population analysis [25]. Note, however, that ionic charges

are not determined experimentally for GaP and their theoretical values depend very much on definition and method of calculation. For instance, the value given in the table was obtained theoretically using a Mulliken scheme [40].

The (110) surface relaxation is usually described in terms of the 'bond rotation model' [1, 30, 42]: the surface bonds rotate without changing their bond lengths appreciably such that surface P (Ga) atoms move outward (inward) relative to the ideal surface plane. According to recent calculations [30, 42] in the relaxed structure, the surface Ga–P bond forms an angle $\omega \simeq 27°$ with the (110) plane. Our calculations (in which only the positions of the first-layer atoms were optimized) predict the same direction of the bond rotation. However, the displacements of the atoms are obtained to be smaller: $\omega = 15°$. The main features of the surface band structure are similar to those calculated by other workers (see [1, 42, 43] and references therein). The one-electron energy gap is 4.86 eV. The charges of ions in the inner (third and fourth) layers of the slab ($\pm 1.02e$) are close to those in the bulk calculation ($\pm 1.07e$), while the ionic charges on the surface are reduced ($\sim \pm 0.73e$) with respect to those in the bulk. The latter agrees with the conclusion made in [7]. As one could expect, the net charges of individual layers (0.03; −0.03; 0.0; 0.0; −0.03; 0.03 per surface unit cell) and the surface charge are close to zero. This result, which is characteristic of non-polar surfaces, changes dramatically for the polar (100) GaP surface as discussed in the next section.

4. Results of calculations

4.1. The slab models of the GaP(100) surface

In this study we are interested in the charge and potential distrubutions near the (100)GaP surface rather then global optimization of the surface structure. Therefore in all further calculations we adopted the same qualitative model for the GaP(100) surface structure as was suggested in recent studies for the GaAs(100) surface (see, for example, [11, 17, 18]). The structures of both As- and Ga-terminated surfaces are usually described in terms of As- and Ga surface dimers [11]. The (100) surface of GaP was modelled by four-layer, eight-layer and ten-layer slabs. In all cases the top of the slab was P terminated and the bottom was Ga terminated. The Ga surface coverage, θ, was fixed to be 2:4 (there were two Ga dimers on the bottom surface). Three P stoichiometries θ = 2:4, 3:4, and 4:4 were studied. This corresponds to two, three, and four surface P dimers per LUC respectively and to 72-, 74-, and 76-atom LUCs in the case of the ten-layer slab. The surface LUC corresponded to the 2×4 extension of the smallest surface unit cell ($a_1 = a_0(2\sqrt{2}, 0)$ and $a_2 = a_0(0, 4\sqrt{2})$). This allows us to study the 2×4 reconstruction of the P-rich and the 4×2 reconstruction of the Ga-rich surfaces [44]. Changes in the surface composition were achived by adding (adsorbing) P dimers to the surface top layer.

Only the relaxation of the top layer was taken into account. As was calculated in [17] for the (100) GaAs surface, the relaxation of the lower surface layers provides only a small contribution to the surface energy. Two coordinates for each surface dimer were independently optimized: the bond distance and the vertical displacement of the dimer relative to the perfect non-relaxed (100) surface. The geometry optimization of the top surface layers was performed for the four- and eight-layer slabs only. The calculated atomic coordinates were practically the same in both calculations. The LUC energies of the eight-layer slab in the four-layer slab geometries are about 0.04 eV higher than those in the independently relaxed eight-layer slab. The atomic structures optimized in the eight-layer slab calculations were then used for the electronic structure (charges and potentials)

calculations in the ten-layer slab.

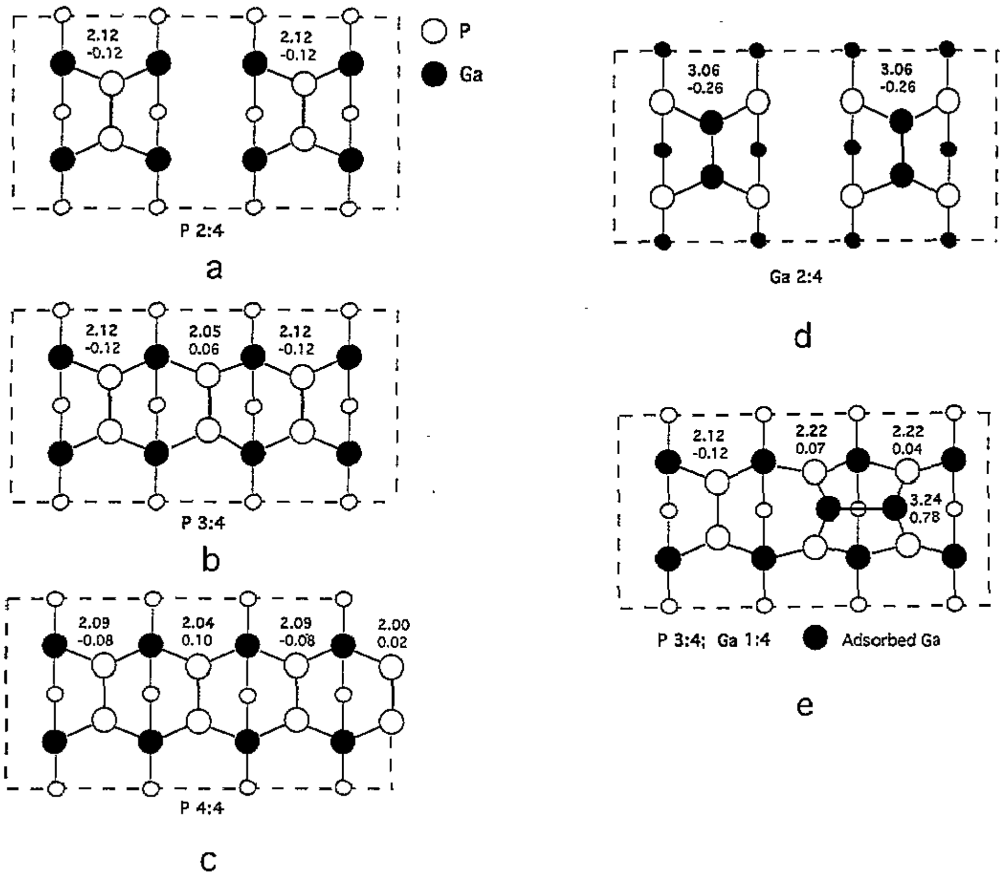

Figure 2. Schematic structures of the surface 2×4 unit cells. Positions of the atoms in the three top surface layers are shown as viewed from above. Smaller circles correspond to the atoms in the third layer. Bonds in the surface dimers (P_2 and Ga_2) are shown by bold lines. The dimer bondlength and its displacement perpendicular to the surface plane with respect to the bulk position are shown by the number beside each dimer where the bondlength is shown in bold. (a) P-terminated surface, stoichiometry 2:4; (b) P-terminated surface, stoichiometry 3:4; (c) P-terminated surface, stoichiometry 4:4; (d) Ga-terminated surface, stoichiometry 2:4; (e) P-terminated 3:4 surface with adsorbed Ga dimer.

4.2. Surface geometry and energetics

The results of the geometry optimization for the eight-layer slab modelling the (100) GaP surface are presented in figure 2. The calculated Ga–Ga and P–P distances are much closer to the molecular bondlengths than to the interatomic distances in the crystal (3.82 Å in our calculations). In particular, the interatomic distances in the surface P dimers (about 2.1 Å) are only slightly longer than the calculated bondlength in the P_2 molecule, 1.87 Å. Thus both P–P and Ga–Ga chemical bonds at the surface resemble those in molecular species. The structure of the block comprising three P dimers (see figure 2(b)) is very similar to that determined theoretically for the GaAs(100) surface [17]. In particular, the central dimer

is displaced out of the ideal surface plane whereas two other dimers displace inside the surface. Note also an alternating character of the displacements of the P dimers in the z direction for the 4:4 surface which is clearly seen in figure 2(c).

The values of the P and Ga dimer desorption energies may be considered as an indicator of the surface stability. We found the P_2 desorption energies to be 5.7 eV, 6.6 eV, and 6.1 eV for the 2:4, 3:4, and 4:4 surfaces respectively. These values may be compared with the As_2 desorption energy from the GaAs(100) surface (3.9 eV) which was estimated from the analysis of the experimental data in [45]. The values for P_2 desorption energies should be higher because the chemical bonding in the GaP crystal is known to be stronger than that in the GaAs crystal [39]. However, this effect is overestimated in our method (see table 5). The fact that the highest desorption energy was obtained for the 3:4 surface agrees with the theoretically predicted high stability of the similar e.g. 'missing-dimer' 3×4 reconstructed GaAs (100) surface [11, 17]. We should note, however, that not only 3:4 'missing-dimer' [31, 46] but also 2:4 'two-missing-dimers' [32, 47] structures were observed in the STM experiments on the GaAs(100) surface.

We also performed calculations of adsorption of up to four Ga atoms on the P-terminated 3:4 and 4:4 surfaces. The surface geometry was optimized assuming that pairs of Ga atoms form dimers on the surface as discussed in [4]. From these calculations we were able to determine the desorption energy of one Ga atom from the surface. This value varies from 5.8 eV to 6.4 eV depending on P and Ga stoichiomentry. Taking into account the stronger bonding in the GaP crystal than that in the GaAs crystal these values are in good agreement with the experimental estimate of the activation energy for Ga atoms desorbing from the GaAs(100) surface; 4.6 eV [23]. The highest desorption energy (6.4 eV) corresponds to one Ga dimer adsorbed on top of the three P dimer block characteristic of the 3:4 surface (see figure 2(e)). Note that this configuration was also predicted to be stable in the EHC model [4].

4.3. Atomic charges and surface potential

The absolute values of the ionic charges calculated for the ten-layer slabs with three P stoichiometries and averaged over each layer are presented in figure 3(a). A similar picture is characteristic also for the eight-layer slab: the charges reach their maximum value 1.01–1.08e in the middle of the slab (see table 6). These values are close to the bulk charges of 1.07e (note that the four-layer slab is not thick enough to reproduce the bulk charges in the middle of the slab). Therefore we conclude that the ions in the interior of both the eight-layer slab (layers 5–6) and the ten-layer slab (layers 5–8) are similar to those in the bulk. The ionic charges differ from those in the bulk in four layers near the (100)P surface and in two layers near the (100)Ga surface. The decrease of the coordination number of the surface ions implies that Ga and P should tend to return to their atomic configurations. Indeed, the charges of ions reduce dramatically in the surface regions, as is clearly seen in figure 3(a). Due to the surface states the one-electron bandgap of the slab, E_g^s, decreases with respect to the bulk value of 4.46 eV. E_g^s = 3.67 eV, 4.28 eV, and 4.41 eV for θ = 2:4, 3:4, and 4:4 respectively. Although more extensive calculations including electron correlation are needed in order to be able to draw final conclusions, we consider its rather high value as an indicator that the surface does not have a metallic character.

The crystalline potential in the bulk region of the slab approaches its value corresponding to the Madelung constant of the 3D zincblende lattice and the bulk ionic charges (see figure 3(b)). However, the electrostatic potential on the ions in the surface region decreases dramatically. This behaviour is consistent with the decrease of ionicity near the surface. It

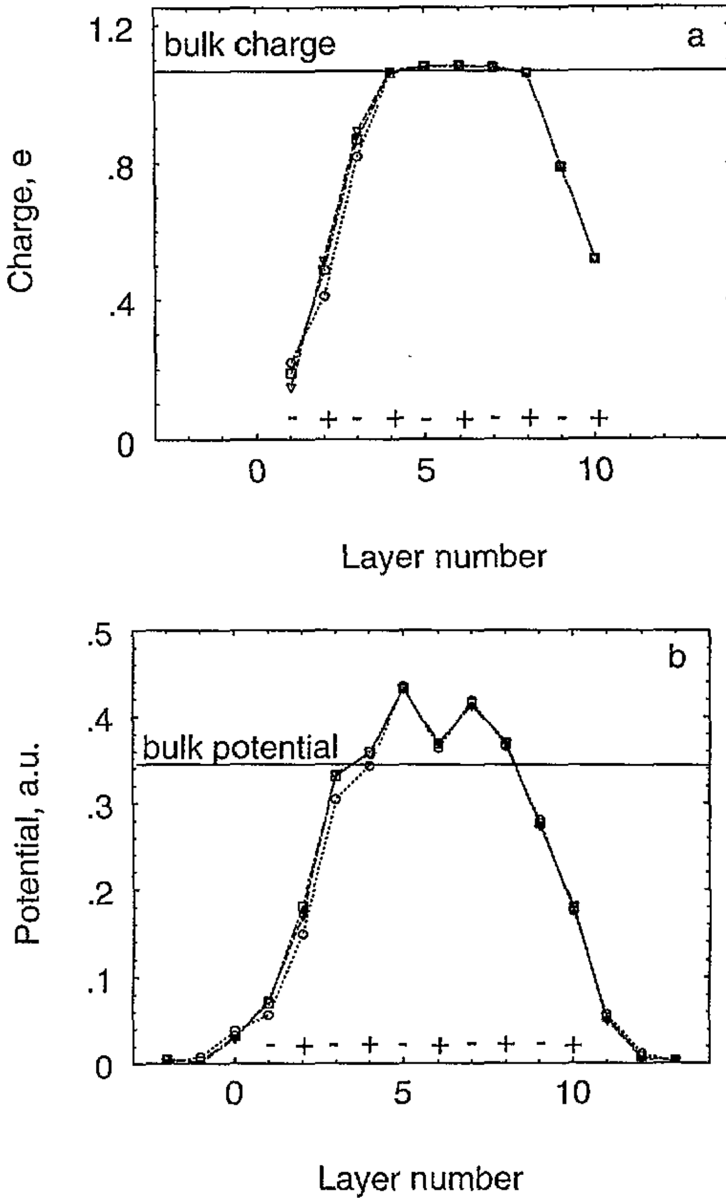

Figure 3. Distribution of absolute values (averaged over each atomic layer) of ionic charges (a) and crystalline potentials (b) on ions and outside the slab for the ten-layer slab. Circles, 2:4 stoichiometry; squares, 3:4 stoichiometry; triangles, 4:4 stoichiometry.

is important that the crystalline potential falls rapidly to practically zero values in vacuum regions on both sides of the slab. According to equation (1) this means that the dipole moment of the slab is close to zero.

The calculated values of the Q_{Ga} and Q_P surface charges (per 2×1 surface unit cell) for the ten-layer slab are presented in table 6. The absolute values of the bulk ionic charges q_b are given for comparison in the same table. The division of the slab into the Ga surface,

Table 6. Surface charges per 2 × 1 unit cell, and the absolute values of the bulk ionic charges for three (100) surface stoichiometries computed in four-, eight-, and ten-layer slab models.

Total number N of layers	Region	Atomic layers	Stoichiometry 2:4	3:4	4:4
4	Ga surface	3–4	−0.53	−0.62	−0.67
	P surface	1–2	0.53	0.62	0.67
	'Bulk'[a]	2–3	0.42	0.49	0.52
8	Ga surface	7–8	−1.02	−1.05	−1.05
	P surface	1–4	1.02	1.05	1.07
	Bulk	5–6	1.01	1.06	1.06
10	Ga surface	9–10	−1.06	−1.06	−1.06
	P surface	1–4	1.07	1.08	1.08
	Bulk	5–8	1.07	1.08	1.08

[a] No bulk region exists in the four-layer slab. The charges averaged over the second and third layers are presented.

P surface, and bulk regions is the same as in section 2. The corresponding divisions for the four- and eight-layer slab are defined in table 6. Note that for this particular division of the slab into the surface and bulk areas the lowest total energy obtained in our calculations corresponds to a non-zero surface charge and zero dipole moment of the slab.

The values of the surface charges presented in table 6 depend, however, on the choice of the bulk region. Suppose, for instance, that instead of the division adopted for the previous discussion (division 1 in figure 1) we chose the surface and bulk regions as follows (division 2 in figure 1): P surface layers 1–3; bulk layers 4–7; Ga surface layers 8–10. In this case the surface charges would become $Q'_{\rm P} \simeq Q_{\rm P} - 2q_{\rm b}$ and $Q'_{\rm Ga} \simeq Q_{\rm Ga} + 2q_{\rm b}$. The charge of the bulk is still zero, but as one can see, these two partitions of the slab correspond to different dipole moments of the bulk region.

To have a completely unambiguous definition of the surface charge, we suggest that the slab is divided in such a way that the dipole moment of the bulk region is equal to zero. It is easy to prove that such partition is always possible if the slab is thick enough and the charge distribution in the inner part of the slab is z periodic. Such a definition (see also [48]) seems preferable since surface charges in this case are closely related to the dipole moment of the slab

$$D \to_{d\to\infty} -Q''_{\rm Ga}d = Q''_{\rm P}d \tag{2}$$

and to the surface potentials (see equation (1)) which are (in principle) experimentally measurable quantities. As is clear from this equation, the surface charge defined in such a way should be zero in order to prevent an infinite increase of the dipole moment of the slab. In the slab model shown in figure 1 the bulk region bearing zero dipole moment (and zero charge) may be defined, for instance, as consisting of whole layers 5–7 and half of the ions in layers 4 and 8. According to this definition of the bulk, the P surface should consist of 1–3 layers and halflayer 4 and the Ga surface is formed from layers 9–10 and half of the layer 8. It can be seen readily that if one calculates the surface charges according to this definition, namely

$$Q''_{\rm P} \approx Q_{\rm P} - q_{\rm b} \qquad Q''_{\rm Ga} \approx Q_{\rm Ga} + q_{\rm b} \tag{3}$$

they appear to be very close to zero. As can be seen in table 6 the accuracy of this result increases as the slab thickness increases.

5. Discussion and conclusions

The qualitative conclusions which can be drawn from our calculations regarding surface charge, ionicity and dipole moment are summarized in table 1 and compared with the main assumptions of other models which were discussed in section 2. First, we should note that despite the fact that the total surface charge and the dipole moment of the slab were found to be the same for the three P surface stoichiometries studied, the electronic density distribution in several subsurface layers depends on the surface composition. This is in contrast with the assumptions of the model theories discussed in section 2. For both (110) and (100) surfaces the electrostatic potential and ionic charges on surface atoms are determined to be less than those in the bulk crystal. Moreover, the charges of individual surface ions vary in a rather broad interval (for instance, from $-0.07e$ to $-0.23e$ for the P atoms in the ten-layer slab) depending on the atomic positions and surface stoichiometry.

The reduced surface ionicity obtained in our calculations (note that the charges on surface ions are smaller than those predicted by the EHC model), implies a mixed P–Ga character of the filled and empty surface bands and partial occupancies of both P and Ga dangling bonds. However, similarly to the main statement of the EHC and Harrison models, the filled (empty) surface bands have predominantly P (Ga) character. Note that due to the mixed character of the surface bands, the partial occupancy of the dangling bonds does not necessarily imply a metallic character of the surface electronic structure. However, more accurate calculations of the band-to-band transitions are needed in order to address this point. The most stable surface structures (see figure 2(b) and 2(e)) obtained in our calculations agree with those predicted in the EHC model.

As was demonstrated in previous studies the EHC rule can be used as a useful tool for qualitative analysis of stability of different possible surface structures. The results of the present work have demonstrated that the charge density distribution near polar surfaces predicted by the EHC model should be corrected taking into account additional factors. In particular, our calculations predict zero dipole moment of the slab, independent of the surface structure and stoichiometry. The condition $D = 0$ seems to be an important criterion of the surface stability. A similar conclusion can be drawn from the NML model (see table 1). However, since the charges of the surface ions are flexible in our model this criterion does not impose such severe restrictions on the surface stoichiometry, composition, and structure as are suggested in the NML model [2]. We stress that structure and stability of polar surfaces are determined by a balance of stoichiometric factors and electron density redistribution which should both be taken into account in a self-consistent manner.

Acknowledgments

This work was carried out as part of the European Economic Community's action 'Human Mobility for Eastern Europe'. EVS is grateful to the Commision of the European Communities for financial support (Contract No ERB-CIPA-CT-92-2189). ALS thanks the Royal Institution of Great Britain for financial support. The authors wish to thank E N Heifets for his contribution at the initial stage of this project, and N Itoh and C R A Catlow for stimulating discussions.

References

[1] Bechstedt F and Enderlein R 1988 *Semiconductor Surfaces and Interfaces* (Berlin: Academie)
[2] Nosker R W, Mark P and Levine J D 1970 *Surf. Sci.* **19** 291

[3] Harrison W A 1979 *J. Vac. Sci. Technol.* **16** 1492
[4] Farrell H H, Harbison J P and Peterson L D 1987 *J. Vac. Sci. Technol.* B **5** 1482
[5] Chadi D J 1991 *The Structure of Surfaces III* (*Springer Series in Surface Science 24*) ed S Y Tong, M A Van Hove, K Takayanagi and X D Xie (Berlin: Springer) p 532
[6] Pashley M D 1989 *Phys. Rev.* B **40** 10481
[7] Pandey K C 1982 *Phys. Rev. Lett.* **49** 223
[8] Tong S Y, Mei W N and Xu G 1984 *J. Vac. Sci. Technol.* B **2** 393
[9] Chadi D J 1984 *Phys. Rev. Lett.* **52** 1911; 1986 *J. Vac. Sci. Technol.* A **4** 944
[10] Lowther J E 1986 *Surf. Sci.* **172** 81
[11] Chadi D J 1987 *J. Vac. Sci. Technol.* A **5** 834
[12] Ren S-F and Chang Y-C 1991 *Phys. Rev.* B **44** 13 573
[13] Appelbaum J A, Baraff G A and Hamann D R 1976 *Phys. Rev.* B **14** 1623
[14] Kaxiras E, Bar-Jam Y, Joannopoulos J D and Pandey K C 1987 *Phys. Rev.* B **35** 9625
[15] Qian G-X, Martin R M and Chadi D J 1988 *Phys. Rev. Lett.* **60** 1962
[16] Chetty N and Martin R M 1992 *Phys. Rev.* B **45** 6074
[17] Ohno T 1993 *Phys. Rev. Lett.* **70** 631
[18] Northrup J E and Froyen S 1993 *Phys. Rev. Lett.* **71** 2276
[19] Platero G, Sanchez-Dehesa J, Tejedor C, Flores F and Munoz A 1986 *Surf. Sci.* **172** 47
[20] Itoh N, Okano A, Hattori K, Kanasaki J and Nakai Y 1993 *Nucl. Instrum. Methods Phys. Res.* B **82** 310
Khoo G S, Ong C K and Itoh N 1993 *Phys. Rev.* B **47** 2031
[21] Tasker P W 1979 *Phil. Mag.* **39** 119
[22] Causa M, Dovesi R, Pisani C and Roetti C 1986 *Phys. Rev.* B **33** 1308
[23] Joyce B A, Zhang J, Shitara T, Neave J H, Taylor A, Armstrong S, Pemble M E, and Foxon C T 1991 *J. Cryst. Growth* **115** 338
[24] Aoyagi Y, Meguro T, Iwai S and Doi A 1991 *Mater. Sci. Eng.* B **10** 121
[25] Pople J A and Beveridge D L 1970 *Approximate Molecular Orbital Theory* (New York: McGraw-Hill)
[26] Shluger A L and Kotomin E A 1981 *Phys. Status Solidi* b **108** 673
Shluger A L 1985 *Theor. Chim. Acta* **66** 355
[27] Stefanovich E, Shidlovskaya E, Shluger A and Zakharov M 1990 *Phys. Status Solidi* b **160** 529
[28] Shluger A L and Stefanovich E V 1990 *Phys. Rev.* B **42** 9664
Shluger A L, Gale J D and Catlow C R A 1992 *J. Phys. Chem.* **96** 10 389
[29] Moliver S S 1992 *J. Phys.: Condens. Matter* **4** 9971
[30] Swarts C A, McGill T C and Goddard W A III 1981 *Surf. Sci.* **110** 400
[31] Pashley M D, Haberern K W and Woodall J M 1988 *J. Vac. Sci. Technol.* B **6** 1468
[32] Bressler-Hill V, Wassermeier M, Pond K, Maboudian R, Briggs G A D, Petroff P M and Weinberg W H 1992 *J. Vac. Sci. Technol.* B **10** 1881
[33] Ornellas F O and Aquino A J A 1991 *Theor. Chim. Acta* **79** 105
[34] Balasubramanian K 1986 *J. Phys. Chem.* **90** 6786
[35] Meier U, Peyerimhoff S D and Grein F 1991 *Chem. Phys.* **150** 331
[36] Gingerich K A and Piacente V 1971 *J. Chem. Phys.* **54** 2498
[37] Evarestov R A 1982 *Quantum-Chemical Methods in Solid State Theory* (Leningrad: Leningrad University Press)
[38] Northrup J E, Ihm J and Cohen M L, *Phys. Rev. Lett.* 1981 **47** 1910
[39] Causa M, Dovesi R and Roetti C 1991 *Phys. Rev.* B **43** 11 937
[40] Huang M-Z and Ching W Y 1985 *J. Phys. Chem. Solids* **46** 977
[41] Vogl P, Hjalmarson H P and Dow J D 1983 *J. Phys. Chem. Solids* **44** 363
[42] Alves J L A, Hebenstreit J and Scheffler M 1991 *Phys. Rev.* B **44** 6188
[43] Whittle R, McGovern I T, Hughes A, Shen T-H and Matthai C C 1993 *J. Phys.: Condens. Matter* **5** 6555
[44] Vitomirov I M, Raisanen A, Brillson L J, Lin C L, McIntruff D T, Kirchner P D and Woodall J M 1993 *J. Vac. Sci. Technol.* A **11** 841
[45] Tsao J Y, Brennan T M, Klem J F and Hammons B E 1989 *J. Vac. Sci. Technol.* A **7** 2138
Kaspi R and Barnett S A 1991 *Surf. Sci.* **241** 146
[46] Gallagher M C, Price R H and Willis R F 1992 *Surf. Sci.* **275** 31
[47] Pashley M D, Haberern K W and Feenstra R M 1992 *J. Vac. Sci. Technol.* B **10** 1874
[48] Tagantsev A K 1991 *Phase Transit.* **35** 119